JOURNAL OF BACTERIOLOGY, Dec. 2007, p. 8503–8509 Vol. 189, No. 23
0021-9193/07/$08.00+0 doi:10.1128/JB.00769-07

Atomic Force Microscopy Study of the Effect of Lipopolysaccharides and Extracellular Polymers on Adhesion of *Pseudomonas aeruginosa*▽

Arzu Atabek and Terri A. Camesano*

Department of Chemical Engineering, Life Sciences and Bioengineering Center, Worcester Polytechnic Institute, 60 Prescott St., Worcester, Massachusetts 01605

Received 17 May 2007/Accepted 14 September 2007

The roles of lipopolysaccharides (LPS) and extracellular polymers (ECP) on the adhesion of *Pseudomonas aeruginosa* PAO1 (expresses the A-band and B-band of O antigen) and AK1401 (expresses the A-band but not the B-band) to silicon were investigated with atomic force microscopy (AFM) and related to biopolymer physical properties. Measurement of macroscopic properties showed that strain AK1401 is more negatively charged and slightly more hydrophobic than strain PAO1 is. Microscopic AFM investigations of individual bacteria showed differences in how the biopolymers interacted with silicon. PAO1 showed larger decay lengths in AFM approach cycles, suggesting that the longer polymers on PAO1 caused greater steric repulsion with the AFM tip. For both bacterial strains, the long-range interactions we observed (hundreds of nanometers) were inconsistent with the small sizes of LPS, suggesting that they were also influenced by ECP, especially polysaccharides. The AFM retraction profiles provide information on the adhesion strength of the biopolymers to silicon (F_{adh}). For AK1401, the adhesion forces were only slightly lower (F_{adh} = 0.51 nN compared to 0.56 nN for PAO1), but the adhesion events were concentrated over shorter distances. More than 90% of adhesion events for AK1401 were at distances of <600 nm, while >50% of adhesion events for PAO1 were at distances of >600 nm. The sizes of the observed molecules suggest that the adhesion of *P. aeruginosa* to silicon was controlled by ECP, in addition to LPS. Steric and electrostatic forces each contributed to the interfacial interactions between *P. aeruginosa* and the silicon surface.

Pseudomonas aeruginosa is a gram-negative opportunistic pathogen that colonizes multiple environments by using natural compounds as energy sources (33). Since *P. aeruginosa* exists naturally in the environment, it is an effective isolate in biodegradation of petroleum hydrocarbons (27, 36). *P. aeruginosa* also causes serious infections, especially in immunocompromised patients; it causes bacteremia in burn victims, bacterial keratitis in soft contact lens users, and chronic lung infections in cystic fibrosis patients (18, 33). Different adhesins and heterogeneity in its surface structures enable the bacterium to attach to various surfaces and avoid immune system components of the host (18). In addition, *P. aeruginosa* has a large genome size, and it secretes several virulence factors, such as secondary metabolites (i.e., pyocyanin) and toxins (13, 45, 50). Its genetic complexity helps it to adapt to different ecological niches (45).

P. aeruginosa strains are motile, express pili, flagella, and lipopolysaccharides (LPS), and secrete extracellular polymers (ECP), which includes polysaccharides (18, 46) and may include proteins, nucleic acids, and membrane vesicles (26). The latter include a mixture of outer membrane proteins, LPS, phospholipids, and periplasmic constituents (6, 35). These molecules are important in the release of extracellular virulence factors, biofilm formation, transport of antibiotics, and cell surface-related properties, such as adhesion and motility (7, 14, 29, 45). Therefore, the development of new vaccines and antimicrobial agents can be aided by the identification and improved characterization of outer membrane proteins, pili, LPS, and ECP.

LPS molecules are present on the outer membranes of gram-negative bacteria with significant variations in coverage, thickness, and local distribution (49). The three components of LPS are lipid A, core polysaccharides, and O-specific chains (12, 39). Characteristics of LPS, such as three-dimensional structure and number of repeating units, contribute to bacterial adhesion (11) and in part, determine cellular physicochemical properties, such as hydrophobicity, interfacial energy, and electrostatic charge (17, 43, 51).

The LPS structure of some strains of *P. aeruginosa* has been well studied. For example, *P. aeruginosa* PAO1 is a genetically well-characterized serotype O5 wild-type strain (18, 45). It is a smooth strain because it expresses the serotype-specific O antigen (B-band) and the common A-band antigen ($A^+ B^+$) (21). *P. aeruginosa* AK1401 (expresses the A-band but not the B band [$A^+ B^-$]), with one repeating saccharide unit (A-band only) that consists of neutral polysaccharides, is a semirough mutant of PAO1 (5, 31). Nuclear magnetic resonance and chemical analyses showed that the core LPS regions of PAO1 and AK1401 were identical (41).

Rivera et al. and Stoica et al. suggest that the A- and B-bands from *P. aeruginosa* PAO1 strain are antigenically and chemically distinct (37, 38, 44). A-band is present in many standard serotype and clinical strains, so it appears to be a common *P. aeruginosa* antigen (35). A-bands lack reactive amino sugars and phosphate; A-bands contain mainly repeating trisaccharides of α-D-rhamnose, with small amounts of ribose, mannose, glucose, and 3-*O*-methylhexose (3). A-band molecules are less negatively charged than B-band molecules

* Corresponding author. Mailing address: Department of Chemical Engineering, Life Sciences and Bioengineering Center, Worcester Polytechnic Institute, 60 Prescott St., Worcester, MA 01605. Phone: (508) 831-5380. Fax: (508) 831-5853. E-mail: terric@wpi.edu.

▽ Published ahead of print on 28 September 2007.

are (37). B-band is the serotype-specific antigen composed of di- to pentasaccharide repeats (9). B-bands contain much longer polysaccharides than A-bands do, and they are concentrated in amino sugars, but low in sulfate and rhamnose (38). The O antigen of strain PAO1 is composed of residues of amino derivatives of uronic acid with a trisaccharide repeating unit of the β-D-manno configuration and *N*-acetyl-D-fucosamine (28, 29). However, the distribution of A- and B-bands on the cell surface is still not clearly known; it is not known whether the LPS types are randomly distributed or present in distinct domains (34). There are still unresolved questions among experts in this field as to whether A-band and B-band molecules are present on adjacent LPS molecules (30, 37) or on the same LPS molecule (22).

P. aeruginosa PAO1 also produces ECP, including anionic polysaccharides that play a role in biofilm formation (52), as well as numerous other compounds, including proteins, nucleic acids, compounds in membrane vesicles, and lipids (24). While few studies have addressed differences in the ECP of strains PAO1 and AK1401, it has been noted that membrane vesicles released by PAO1 contained more protein than membrane vesicles released by AK1401 (35).

In our study, we used atomic force microscopy (AFM) to characterize the physical properties of bacterial surface molecules (LPS and ECP) associated with *P. aeruginosa* PAO1 and AK1401. Macroscopic tests, such as zeta potential and contact angle measurements, were also used to help characterize the bacterial surfaces. AFM was used to measure the forces of adhesion between the bacterial strains and a model surface, silicon. We then correlated the direct measurements of adhesion force with information on the physical properties of the surface molecules of these two bacterial strains.

MATERIALS AND METHODS

Bacterial culture conditions. Two strains of *Pseudomonas aeruginosa*, smooth PAO1 ($A^+ B^+$) and semirough AK1401 ($A^+ B^-$), were provided by Gerald Pier (Channing Laboratory, Department of Medicine, Brigham and Women's Hospital, Harvard Medical School). Cultures were maintained at 4°C on tryptic soy agar (TSA) (Sigma-Aldrich, St. Louis, MO). Tryptic soy broth (TSB) (Sigma-Aldrich, St. Louis, MO) was used as the liquid growth medium. Strains PAO1 and AK1401 were grown in TSB to mid-exponential phase (optical density at 600 nm of 0.9) at 37°C. All experiments were performed in ultrapure water (Millipore, Billerica, MA) or in HEPES buffer (Sigma-Aldrich, St. Louis, MO) (50 mM HEPES, 110 mM NaCl, pH 7.4).

Bacterial cell attachment to clean glass slides. Micro cover glass slides (VWR International, West Chester, PA) were cleaned with a 4:1 mixture of H_2SO_4 and H_2O_2, respectively. They were kept in the acid solution for 25 min and then rinsed with ultrapure water.

Bacterial cell suspensions were centrifuged at 3,500 × *g* for 15 min. The supernatant was eluted, and the pellet was washed once with ultrapure water and resuspended in ultrapure water. Differences in the bacterial surfaces made it necessary to use two protocols to bond bacteria to the slides. The binding protocol used for strain AK1401 involves a 1-ethyl-3-(3-dimethylaminopropyl) carbodiimide hydrochloride (EDC)–*N*-hydroxysuccinimide (NHS) cross-linking reaction and has been used extensively in our laboratory for *Pseudomonas putida* immobilization to glass (2). For strain PAO1, poly-L-lysine (PLL) was used to attach bacteria to the slides. In another study, we systematically evaluated the binding of bacteria, including *P. aeruginosa*, to glass slides using the EDC-NHS reaction, PLL attachment, and mechanical trapping (32). All three methods resulted in similar bacterial images and similar force profiles with the AFM.

(i) Attachment of *P. aeruginosa* AK1401. The clean glass slides were treated with ethanol for 5 min and then treated with methanol for 5 min. The glass slides were incubated in 10% aminosilane (3-aminopropyl dimethoxysilane; Sigma-Aldrich, St. Louis, MO) solution in methanol for 15 min. The glass slides were rinsed with 50 ml of methanol and then with 25 ml of water and kept in methanol until the bacterial suspension was added to the slides. The cell suspension was treated with 300 μl of 100 mM EDC (Pierce Cellomics, Rockford, IL) at pH 5.5 and left to equilibrate for 3 min. The treatment with EDC was followed by the addition of 300 μl of 40 mM *N*-hydroxysulfosuccinimide (Sulfo-NHS) (Pierce Cellomics, Rockford, IL) at pH 7.5 to the mixture. The bacterial suspension with EDC–Sulfo-NHS was equilibrated for 10 min and added to the aminosilane-treated clean glass slides. The glass slides with bacterial suspension were agitated for 12 h at 70 rpm at room temperature to promote bacterial attachment.

(ii) Attachment of *P. aeruginosa* PAO1. Clean glass slides were soaked in 100 μl of 0.1% (wt/vol) PLL solution (Sigma-Aldrich, St. Louis, MO), and the PLL solution was allowed to dry for 2 h. Then, the bacterial suspension in water was added to PLL-treated glass slides and kept on the shaker at 70 rpm for 2 h to promote bacterial attachment.

Bacterial interaction and adhesion force measurements with AFM. A Dimension 3100 atomic force microscope with Nanoscope IIIa controller (Veeco Metrology, Inc., Santa Barbara, CA) was used. CSC38-B type silicon cantilevers (Mikromasch, Wilsonville, OR) were used for all force curve measurements. According to the manufacturer, the radius of these tips is <10 nm.

Spring constants (k_c) were measured using a thermal technique (8). Five noise spectra were captured for each cantilever before and after the AFM experiments, and the k_c values from each spectrum were calculated and averaged. We used a different tip for each experiment and measured the k_c each time. The average k_c value was 0.16 ± 0.08 N · m^{-1} ($n = 30$).

Interactions of *P. aeruginosa* with silicon were investigated by AFM in HEPES buffer. Ten different bacterial cells were tested, and five force curves were captured for each cell. The approach and retraction portions of the AFM force profiles were captured. The deflection voltage-separation distance curves were converted into force versus separation curves (force measured in nanonewtons, and separation measured in nanometers) (15). The pulling rate was constant at 2.39 μm/s for all experiments.

Bacterial physicochemical characterizations. (i) Contact angle measurements. Bacteria were harvested at mid-exponential growth phase and washed three times with HEPES buffer and resuspended in the same solution. Four milliliters of the bacterial cell suspension was poured onto a 0.45-μm filter (membrane filters; Millipore, Billerica, MA) and vacuum filtered. The filters (containing $>10^8$ cells · mm^{-2}) were dried for 45 min, which was determined to be the optimum drying time for the bacterial lawn (20). Subsequently, contact angle measurements were taken at room temperature for water, diiodomethane, and formamide using a goniometer (model 100-00; Ramé-Hart, Netcong, NJ) by the sessile drop technique. Eight filters were prepared for each *P. aeruginosa* strain, and contact angle values were averaged and used for surface free energy calculations (10).

(ii) Zeta potential measurements. A Zetasizer Nano ZS (Malvern Instruments, Southborough, MA) and disposable folded capillary cells (Malvern Instruments, Southborough, MA) were used to measure the zeta potentials (ζ) of the bacterial suspensions at room temperature, using the Smoluchowski equation (16). Bacteria were washed once with HEPES buffer and resuspended in the same solution. For strain AK1401 only, we also measured the ζ values on bacteria that had been treated with the EDC-NHS procedure used for bacterial attachment to the slides, since EDC and NHS were added into the solution with the bacteria during that process, and may have affected the ζ values. We did not consider the effect of PLL on the zeta potential of strain PAO1, because PLL was never added into the bacterial solution but was only on the glass slide. The zeta potentials of all samples were measured six times and averaged.

(iii) Surface free energy calculations. Interfacial interactions, such as Lifshitz-van der Waals (LW) and Lewis acid-base (AB) interactions, govern the initial steps of bacterial adhesion (25). LW interactions are apolar, whereas AB interactions are polar and comprise all electron-acceptor and electron-donor interactions (48). The apolar and polar components of the interfacial free energy are additive and can be described as shown below in equations 1 and 2 (48):

$$\gamma_i = \gamma_i^{LW} + \gamma_i^{AB} \quad (1)$$

$$\gamma_i^{AB} = 2\sqrt{\gamma_i^+ \gamma_i^-} \quad (2)$$

where γ_i is the total surface free energy of component i, γ_i^{LW} is the LW component of the surface free energy, γ_i^{AB} is the AB component of the surface free energy, and γ_i^+ and γ_i^- are the electron acceptor and donor components, respectively.

Young developed an expression to describe the connection between adhesion and the surface tension of a solid (γ_S) and a liquid (γ_L) by using the interfacial tension between solid and liquid (γ_{SL}), and the contact angle (θ) made by a drop of liquid L (48). The Dupré equation expresses the relation between the work of

TABLE 1. Bacterial surface properties measured at room temperature

P. aeruginosa strain	Physicochemical properties									
	Contact angle[a] (°)			Surface energy component[b] (mJ/m^2)					ζ[c] (mV) in:	
	θ^W	θ^D	θ^F	γ_i^{LW}	γ_i^+	γ_i^-	γ_i^{AB}	γ_i	HEPES buffer	HEPES buffer after EDC-NHS exposure
PAO1	31 ± 1	45 ± 2	51 ± 1	26.0	0.21	66.8	7.54	33.6	−13.1 ± 1.00	NA
AK1401	34 ± 1	52 ± 1	46 ± 1	23.6	1.37	56.1	17.5	41.1	−18.9 ± 1.27	−18.5 ± 1.63

[a] θ^W, θ^D, and θ^F are the contact angles of water, diiodomethane, and formamide on *P. aeruginosa*, respectively. The values are the means ± standard deviations from eight filters.

[b] γ_i^{LW} and γ_i^{AB} (γ_i^+ and γ_i^- are electron acceptor and donor components, respectively) are Lifshitz-van der Waals and Lewis acid-base surface free energy components of *P. aeruginosa*, respectively.

[c] The zeta potential (ζ) values are means ± standard deviations from six measurements. NA, not applicable (only strain AK1401 was exposed to EDC-NHS during the cell attachment protocol).

adhesion between a solid and a liquid (48). Inserting the Dupré equation into the Young equation, and combining them with the expressions for apolar and polar interactions, a more precise expression, the Young-Dupré equation (equation 3), can be obtained (48).

$$\gamma_L(1 + \cos\theta) = 2\left(\sqrt{\gamma_S^{LW}\gamma_L^{LW}} + \sqrt{\gamma_S^+\gamma_L^-} + \sqrt{\gamma_S^-\gamma_L^+}\right) \quad (3)$$

RESULTS

Physicochemical bacterial surface properties. According to the water contact angle measurements, *P. aeruginosa* AK1401, with a water contact angle value of 34° ± 1°, was slightly more hydrophobic than *P. aeruginosa* PAO1, with a water contact angle value of 31° ± 1° (Table 1). The total surface free energies of strains PAO1 and AK1401 were similar (Table 1), although AK1401 shows a more dominant acid-base characteristic than strain PAO1 does. The ζ values indicated that AK1401 was more electrostatically negative than PAO1 and that the EDC-NHS treatment did not alter the surface charge of the bacteria (Table 1).

AFM force curve analysis. The AFM analyses provide us with two types of information, depending on whether the data were collected during the tip approach or retraction phase. As the AFM tip is approaching the bacteria, steric repulsive forces are typically observed, and the examination of these profiles provides information on the size of the polymers present on the bacterial surfaces. *P. aeruginosa* PAO1 approach profiles demonstrated a larger decay length (L_o) than did the profiles of AK1401, which was likely due to steric repulsion caused by long polymer chains (Fig. 1A and 2A). The force at zero distance (F_o) was greater for PAO1 than for AK1401 (Fig. 2B).

Analysis of the retraction profiles provides information on the strength of adhesion between the bacteria and the tip, but it can also provide information on the length or extension of the bacterial polymers. As the tip is brought into contact with the bacterium, often, some polymers from the surface of the bacterium attach to the probe, and their detachment occurs as the tip is being retracted. These events, which are referred to as "pull-off events," occurred multiple times within a single retraction step for each bacterium (Fig. 1B), which could have represented multiple polymer chains or binding with multiple sites on a single chain. It seems more likely that we observed multiple unfolding events within a single polymer chain, because the force does not return to zero in between adjacent adhesion peaks. Examination of these retraction curves provides a quantitative measure of the strength of adhesion between the bacterium and the probe. The strongest interactions, with a maximum attractive magnitude of ~1 nN, occurred at shorter distances from the surface for strain AK1401 than for strain PAO1 (Fig. 1B). In previous investigations, a single

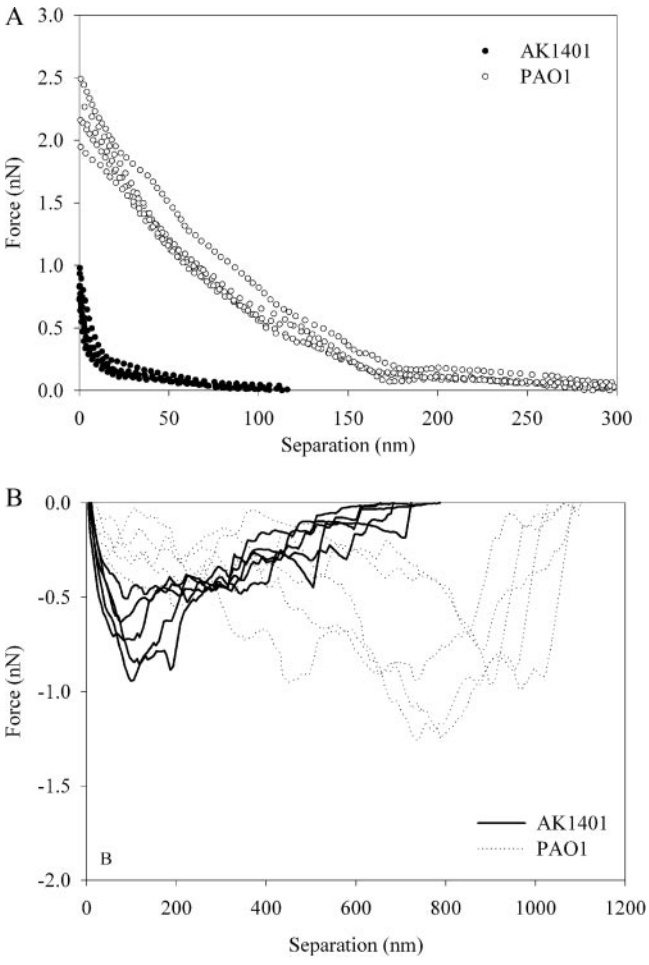

FIG. 1. (A) Representative AFM approach and (B) retraction curves of *P. aeruginosa* strains AK1401 and PAO1. Five data sets that represent typical data obtained for five bacteria are shown. In total, 10 bacteria were examined per condition, and five measurements were made over the center of each cell.

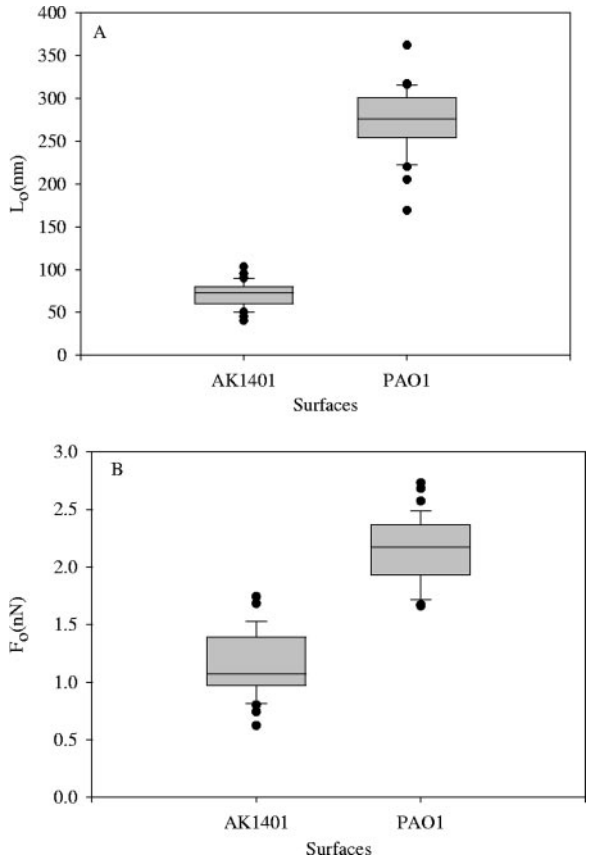

FIG. 2. Box plots showing the median and distribution of the decay length (L_o) (A) and the repulsive force at zero distance (F_o) (B) for *P. aeruginosa* strains from AFM approach curves.

sharp peak was observed when there was no polymer in the system, such as when probing a clean glass slide (4).

The distributions of the pull-off distances for *P. aeruginosa* showed evidence of much longer polymers for strain PAO1 than for strain AK1401 (Fig. 3A). The median L_o values were 567 nm and 320 nm, for PAO1 and AK1401, respectively. The pull-off distances do not directly tell the length of the polymers, but they are related to both polymer length and to how much the polymer can be stretched by the AFM tip.

For strain AK1401, the adhesion forces were of a slightly lower magnitude, both in terms of the average force of adhesion (F_{adh} = 0.51 nN for AK1401 compared to F_{adh} = 0.56 nN for PAO1), and in terms of the distribution of adhesion force values (Fig. 3B). Only strain PAO1 showed high adhesion force values, which were >1.2 nN. However, considering only the average value or the magnitude of the force is misleading because the retraction force profiles showed very different behavior in terms of the distance at which the pull-off events occurred. For example, >90% of adhesion events for AK1401 were at distances of <600 nm, while >50% of adhesion events for PAO1 were at distances of >600 nm (Fig. 3C). The sizes of the molecules observed in the pull-off events are large enough that they must represent ECP, in addition to contributions from LPS molecules.

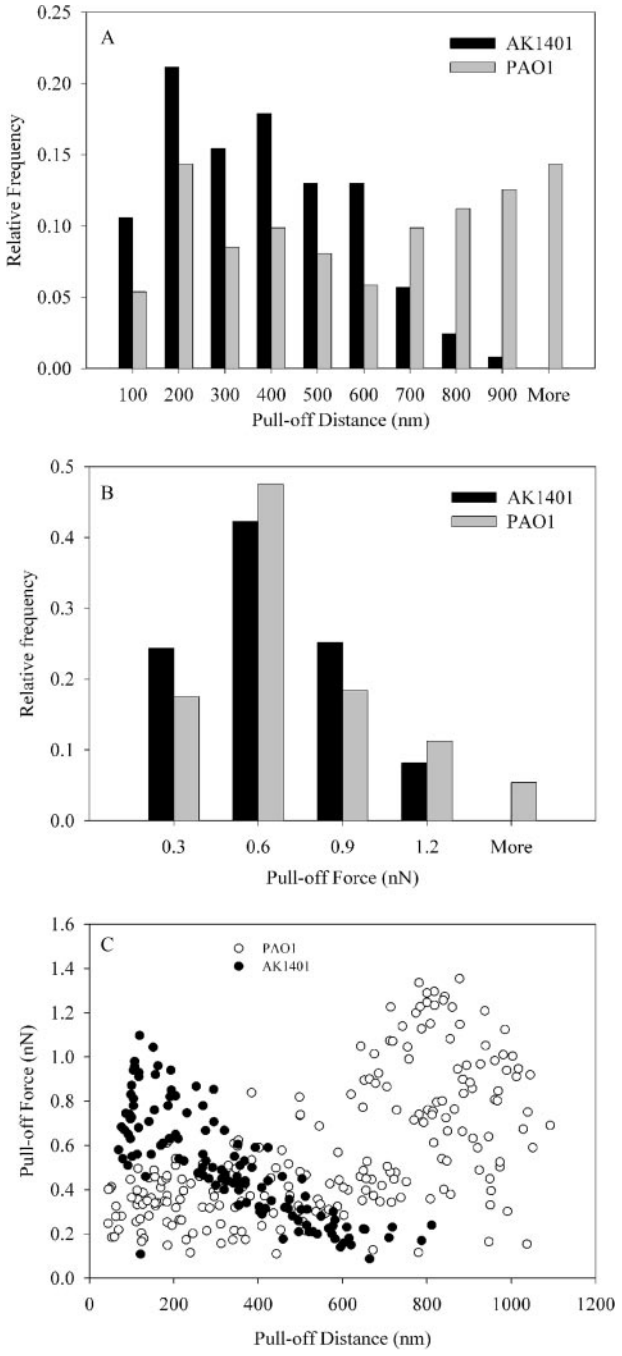

FIG. 3. Histograms showing the distributions of the pull-off distances (A) and pull-off forces (B) (n = 30 for each) of *P. aeruginosa* strains with clean silicon AFM tips. (C) Compilation of all of the adhesion peaks observed in the retraction profiles.

DISCUSSION

AFM analysis of bacterial interaction forces. The EDC-NHS reaction and PLL coating methods were used to immobilize bacteria for AFM experiments. These procedures have been used successfully with bacteria, including *P. aeruginosa* (2, 11, 46). The EDC-NHS reaction can be used to attach bacteria because the reaction targets the surface carboxyl groups (32).

After the EDC-NHS reaction, carboxylic terminal groups on the bacteria form an intermediate complex that is very unstable. If the functional groups on the bacterial surface cannot contact the amine groups on the substrate, they will rapidly revert to their original carboxylate form (23). Therefore, the carboxyl groups that are modified are all on the underside of the bacteria (linking them to the glass). The lack of surface modification caused by the EDC-NHS addition was supported by the nearly identical zeta potentials for *P. aeruginosa* AK1401 that were exposed to these two chemicals and untreated bacteria.

For strain PAO1, PLL was used to help bacteria attach to glass slides. The bacterial surface molecules that interacted with PLL remain on the underside of the bacteria, and there was no excess PLL in solution to interact with the bacteria. Therefore, we did not observe artifacts in our force measurements, which were always made on top of the bacteria. The appropriateness of these two methods was discussed in our previous work, where we showed that bacteria immobilized for AFM experiments through the EDC-NHS reaction, PLL adsorption, or mechanical trapping all exhibited similar properties in the AFM images and force measurements (32).

Roles of bacterial LPS and ECP on interaction profiles. The repulsive forces observed from the AFM approach profiles are likely a combination of steric repulsion from the long extracellular molecules, with some electrostatic contribution for strain PAO1, which may be attributable to the negatively charged B-band LPS molecules. In addition, the ECP of *P. aeruginosa* is anionic (52) and may have had an electrostatic interaction with silicon. It is often impossible to separate the effects of LPS and the other polymers, because as previously noted, the O side chains of PAO1 seem to form an integrated continuum with bacterial ECP (24). For strain AK1401, the LPS has only neutral side chain polysaccharides (A-bands), so the repulsive forces at zero distance (F_o) must be caused by steric interactions or by electrosteric effects from the extracellular polymers. The repulsive forces of strain PAO1 were greater than those of strain AK1401, presumably because strain PAO1 has negatively charged O-side chain polysaccharides (B-bands).

The decay lengths from AFM approach curves can be related to the lengths of the surface polymers of bacteria (2, 11), but an exact determination is difficult, particularly when there is strong electrosteric repulsion (11). Specifically, when the repulsion is stronger, the decay length from the approach curves becomes larger and less representative of the physical length of the bacterial surface polymers. The decay length of strain PAO1 ($L_o = 275 \pm 38$ nm) was longer than that of strain AK1401 ($L_o = 71 \pm 15$ nm).

In the AFM retraction profiles, both *P. aeruginosa* strains showed several adhesion peaks with different magnitudes, indicating that multiple binding sites on single polymers or that several different polymers might be involved in determining the total interactions with silicon. The fact that the interactions occurred over such a long range also indicated that the polymers are elastic and might be coiled on the bacterial surface, becoming unfolded as they were pulled with the AFM tip. The large sizes suggest that LPS alone cannot be responsible for causing the adhesive interactions, since no studies have shown such large LPS molecules. The common antigen (A-band) polymer is comprised of 10 to 20 repeating α-D-rhamnose units (3). Strain PAO1, in addition to expressing A-bands, has 30 to 50 O-repeating units of B-band polymer, with an approximate length of 39 to 65 nm (29). Prior research was unable to determine whether the O chains were extended or coiled on the bacterial surfaces (29). Pili have also been found to be an important contributor to long-range interactions observed from AFM force profiles. For example, an AFM investigation of PAO1 showed that type IV pili were responsible for large pull-off distances, reaching 400 to 3,000 nm (46). In extensive AFM imaging of the *P. aeruginosa* strains that were grown under the conditions of the present study, we never observed pili in the images (1, 4). Therefore, on the basis of the molecular sizes we observed from the AFM measurements and because we did not detect any pili, ECP were the most likely molecules to have interacted with the tip during the adhesion events that occurred in the range of hundreds of nanometers.

In a previous work, we extracted the ECP from strains PAO1 and AK1401 through several centrifugation, supercentrifugation, and ultracentifugation steps with washing in between. We found that the supernatant material, when dried on a glass slide, formed 120-nm clusters for PAO1 but 17-nm clusters for AK1401 (4). Although the ECP may contain proteins, the sizes of the molecules observed and the magnitude of the forces measured in the AFM investigations are more consistent with what has been observed in other studies of exopolysaccharides, such as forces that decayed at distances of ≥1,000 nm for ECP isolated from *Pseudomonas atlantica* (19).

Physicochemical bacterial surface properties. The macroscopic measurements of bacterial zeta potential and contact angle do not provide enough information to explain the interaction profiles and adhesion forces measured by AFM. *P. aeruginosa* AK1401 is slightly more hydrophobic than *P. aeruginosa* PAO1 is, according to the water contact angle measurements. However, the total surface free energies of strain PAO1 and strain AK1401 were relatively similar and also close to values observed for many other types of gram-negative and gram-positive bacteria (42). Surface free energy components include only Lifshitz-van der Waals and Lewis acid-base interactions. In this study, electrostatic and steric interactions appeared to dominate the bacterial interaction force profiles observed. A previous investigation of the surface hydrophobicity of *P. aeruginosa* strains, measured by hydrophobic interaction chromatography, showed that the hydrophobicities could be ranked as follows: $A^+ B^-$ (AK1401) > $A^- B^-$ > $A^+ B^+$ (PAO1) > $A^- B^+$ (34). In another study, B-band LPS were hypothesized to influence the initial attachment of the bacterium to hydrophilic surfaces, since the presence of the B-band made the strains more hydrophilic (40).

Previous work showed that *P. aeruginosa* cells lacking B-band LPS had higher surface electronegativity than strain PAO1, which the authors attributed to the core region of the LPS holding most of the groups determining surface charge (34). In our experiments, we confirmed that strain AK1401 was more electostatically negative than PAO1 was, but we cannot rule out the possibility that differences in ECP produced by these two strains could have contributed to the differences in zeta potential, rather than an effect due to exposure of the core and lipid A region for AK1401.

In summary, since physicochemical bacterial surface properties are calculated from the macroscopic scale, not for an

individual bacterium, they are similar for both strains. However, the AFM measurements go beyond the single-cell level, and in fact, we are measuring the properties of individual molecules or small groups of molecules. For this reason, AFM results often cannot be explained with simple correlations of bacterial physicochemical properties based on macroscopic assays (47). The AFM investigations of *P. aeruginosa* LPS and ECP suggested that both types of molecules are very important in influencing the interfacial behavior of the bacteria, particularly due to electrostatic and steric interactions.

ACKNOWLEDGMENTS

This research was supported by National Science Foundation (BES-0238627).

The assistance of Paola Pinzon-Arango, Yatao Liu, Jochen Weiss, and Thrandur Helgason with the zeta potential and contact angle measurements is gratefully acknowledged. We also thank David S. Adams, Ray J. Emerson IV, Nancy Burnham, Elizabeth Ryder, and Laila Abu-Lail for helpful discussions during the course of these studies, and Joshua Strauss for his comments on a previous version of the manuscript.

REFERENCES

1. **Abu-Lail, L. I.** 2006. An atomic force microscopy study of bacterial adhesion to natural organic matter-coated surfaces in the environment. M.S. thesis. Worcester Polytechnic Institute, Worcester, MA.
2. **Abu-Lail, N. I., and T. A. Camesano.** 2003. Role of ionic strength on the relationship of biopolymer conformation, DLVO contributions, and steric interactions to bioadhesion of *Pseudomonas putida* KT2442. Biomacromolecules **4:**1000–1012.
3. **Arsenault, T. L., D. W. Hughes, D. B. MacLean, W. A. Szarek, A. M. B. Kropinski, and J. S. Lam.** 1991. Structural studies on the polysaccharide portion of A-band lipopolysaccharide from a mutant (AK1401) of *Pseudomonas aeruginosa* strain PAO1. Can. J. Chem. **69:**1273–1280.
4. **Atabek, A.** 2006. Investigating bacterial outer membrane polymers and bacterial interactions with organic molecules using atomic force microscopy. M.S. thesis. Worcester Polytechnic Institute, Worcester, MA.
5. **Berry, D., and A. M. Kropinski.** 1986. Effect of lipopolysaccharide mutations and temperature on plasmid transformation efficiency in *Pseudomonas aeruginosa*. Can. J. Microbiol. **32:**436–438.
6. **Beveridge, T. J.** 1999. Structures of gram-negative cell walls and their derived membrane vesicles. J. Bacteriol. **181:**4725–4733.
7. **Bryan, L. E., K. O'Hara, and S. Wong.** 1984. Lipopolysaccharide changes in impermeability-type aminoglycoside resistance in *Pseudomonas aeruginosa*. Antimicrob. Agents Chemother. **26:**250–255.
8. **Burnham, N. A., X. Chen, C. S. Hodges, G. A. Matei, E. J. Thoreson, C. J. Roberts, M. C. Davies, and S. J. B. Tendler.** 2003. Comparison of calibration methods for atomic-force microscopy cantilevers. Nanotechnology **14:**1–6.
9. **Burrows, L. L., D. F. Charter, and J. S. Lam.** 1996. Molecular characterization of the *Pseudomonas aeruginosa* serotype O5 (PAO1) B-band lipopolysaccharide gene cluster. Mol. Microbiol. **22:**481–495.
10. **Busscher, H. J., A. H. Weerkamp, H. C. van der Mei, A. W. van Pelt, H. P. de Jong, and J. Arends.** 1984. Measurement of the surface free energy of bacterial cell surfaces and its relevance for adhesion. Appl. Environ. Microbiol. **48:**980–983.
11. **Camesano, T. A., and B. Logan.** 2000. Probing bacterial electrosteric interactions using atomic force microscopy. Environ. Sci. Technol. **34:**3354–3362.
12. **Caroff, M., and D. Karibian.** 2003. Structure of bacterial lipopolysaccharides. Carbohydr. Res. **338:**2431–2447.
13. **Cox, C. D.** 1986. Role of pyocyanin in the acquisition of iron from transferrin. Infect. Immun. **52:**263–270.
14. **Donlan, R. M.** 2000. Role of biofilms in antimicrobial resistance. ASAIO J. **46:**S47–S52.
15. **Ducker, W. A., and T. J. Senden.** 1992. Measurement of forces in liquids using a force microscope. Langmuir **8:**1831–1836.
16. **Elimelech, M., J. Gregory, X. Jia, and R. A. Williams.** 1998. Particle deposition and aggregation: measuring, modelling and simulation. Butterworth-Heinemann, Woburn, MA.
17. **Farley, M. M., W. M. Shafer, and J. K. Spitznagel.** 1988. Lipopolysaccharide structure determines ionic and hydrophobic binding of a cationic antimicrobial neutrophil granule protein. Infect. Immun. **56:**1589–1592.
18. **Fletcher, M.** 1996. Bacterial adhesion: molecular and ecological diversity. Wiley, New York, NY.
19. **Frank, B. P., and G. Belfort.** 1997. Intermolecular forces between extracellular polysaccharides measured with the atomic force microscope. Langmuir **13:**6234–6240.
20. **Gallardo-Moreno, A. M., Y. Liu, M. L. González-Martín, and T. A. Camesano.** 2006. Atomic force microscopy analysis of bacterial surface morphology before and after cell washing. J. Scan. Probe Microsc. **1:**1–11.
21. **Hancock, R. E., and A. M. Carey.** 1979. Outer membrane of *Pseudomonas aeruginosa*: heat- and 2-mercaptoethanol-modifiable proteins. J. Bacteriol. **140:**902–910.
22. **Hatano, K., J. B. Goldberg, and G. B. Pier.** 1993. *Pseudomonas aeruginosa* lipopolysaccharide: evidence that the O side chains and common antigens are on the same molecule. J. Bacteriol. **175:**5117–5128.
23. **Hermanson, G. T.** 1996. Bioconjugate techniques. Academic Press, San Francisco, CA.
24. **Hunter, R. C., and T. J. Beveridge.** 2005. High-resolution visualization of *Pseudomonas aeruginosa* PAO1 biofilms by freeze-substitution transmission electron microscopy. J. Bacteriol. **187:**7619–7630.
25. **Israelachvili, J.** 1992. Intermolecular and surface forces, 2nd ed. Academic Press, London, England.
26. **Kadurugamuwa, J. L., and T. J. Beveridge.** 1995. Virulence factors are released from *Pseudomonas aeruginosa* in association with membrane vesicles during normal growth and exposure to gentamicin: a novel mechanism of enzyme secretion. J. Bacteriol. **177:**3998–4008.
27. **Kahraman, H., and H. Geckil.** 2005. Degradation of benzene, toluene and xylene by *Pseudomonas aeruginosa* engineered with the *Vitreoscilla* hemoglobin gene. Eng. Life Sci. **5:**363–368.
28. **Knirel, Y. A., E. V. Vinogradov, N. A. Kocharova, R. A. Paramonov, N. K. Kochetkov, B. A. Dmitriev, E. S. Stanislavsky, and B. Lanyi.** 1988. The structure of O-specific polysaccharide and serological classification of *Pseudomonas aeruginosa*. Acta Microbiol. Hungarica **35:**3–24.
29. **Lam, J. S., L. L. Graham, J. Lightfoot, T. Dasgupta, and T. J. Beveridge.** 1992. Ultrastructural examination of the lipopolysaccharides of *Pseudomonas aeruginosa* strains and their isogenic rough mutants by freeze-substitution. J. Bacteriol. **174:**7159–7167.
30. **Lam, M. Y., E. J. McGroarty, A. M. Kropinski, L. A. MacDonald, S. S. Pedersen, N. Hoiby, and J. S. Lam.** 1989. Occurrence of a common lipopolysaccharide antigen in standard and clinical strains of *Pseudomonas aeruginosa*. J. Clin. Microbiol. **27:**962–967.
31. **Lightfoot, J., and J. S. Lam.** 1991. Molecular cloning of genes involved with expression of A-band lipopolysaccharide, an antigenically conserved form, in *Pseudomonas aeruginosa*. J. Bacteriol. **173:**5624–5630.
32. **Liu, Y., and T. A. Camesano.** Immobilizing bacteria for atomic force microscopy imaging or force measurements in liquids. ACS Symp. Ser., in press.
33. **Lyczak, J. B., C. L. Cannon, and G. B. Pier.** 2000. Establishment of *Pseudomonas aeruginosa* infection: lessons from a versatile opportunist. Microbes Infect. **2:**1051–1060.
34. **Makin, S. A., and T. J. Beveridge.** 1996. The influence of A-band and B-band lipopolysaccharide on the surface characteristics and adhesion of *Pseudomonas aeruginosa* to surfaces. Microbiology **142:**299–307.
35. **Nguyen, T. T., A. Saxena, and T. J. Beveridge.** 2003. Effect of surface lipopolysaccharide on the nature of membrane vesicles liberated from the Gram-negative bacterium *Pseudomonas aeruginosa*. J. Electron Microsc. **52:**465–469.
36. **Ojumu, T. V., O. O. Bello, J. A. Sonibare, and B. O. Solomon.** 2005. Evaluation of microbial systems for bioremediation of petroleum refinery effluents in Nigera. Afr. J. Biotechnol. **4:**31–35.
37. **Rivera, M., L. E. Bryan, R. E. Hancock, and E. J. McGroarty.** 1988. Heterogeneity of lipopolysaccharides from *Pseudomonas aeruginosa*: analysis of lipopolysaccharide chain length. J. Bacteriol. **170:**512–521.
38. **Rivera, M., and E. J. McGroarty.** 1989. Analysis of a common-antigen lipopolysaccharide from *Pseudomonas aeruginosa*. J. Bacteriol. **171:**2244–2248.
39. **Rocchetta, H. L., L. L. Burrows, and J. S. Lam.** 1999. Genetics of O-antigen biosynthesis in *Pseudomonas aeruginosa*. Microbiol. Mol. Biol. Rev. **63:**523–553.
40. **Sabra, W., H. Lunsdorf, and A. P. Zeng.** 2003. Alterations in the formation of lipopolysaccharide and membrane vesicles on the surface of *Pseudomonas aeruginosa* PAO1 under oxygen stress conditions. Microbiology **149:**2789–2795.
41. **Sadovskaya, I., J. R. Brisson, J. S. Lam, J. C. Richards, and E. Altman.** 1998. Structural elucidation of the lipopolysaccharide core regions of the wild-type strain PAO1 and O-chain-deficient mutant strains AK1401 and AK1012 from *Pseudomonas aeruginosa* serotype O5. Eur. J. Biochem. **255:**673–684.
42. **Sharma, P. K., and K. H. Rao.** 2002. Analysis of different approaches for evaluation of surface energy of microbial cells by contact angle goniometry. Adv. Colloid Interface Sci. **98:**341–463.
43. **Simoni, S. F., T. N. P. Bosma, H. Harms, and A. J. B. Zehnder.** 2000. Bivalent cations increase both the subpopulation of adhering bacteria and their adhesion efficiency in sand columns. Environ. Sci. Technol. **34:**1011–1017.
44. **Stoica, O., A. Tuanyok, X. Yao, M. H. Jericho, D. Pink, and T. J. Beveridge.** 2003. Elasticity of membrane vesicles isolated from *Pseudomonas aeruginosa*. Langmuir **19:**10916–10924.
45. **Stover, C. K., X. Q. Pham, A. L. Erwin, S. D. Mizoguchi, P. Warrener, M. J.**

Hickey, F. S. Brinkman, W. O. Hufnagle, D. J. Kowalik, M. Lagrou, R. L. Garber, L. Goltry, E. Tolentino, S. Westbrock-Wadman, Y. Yuan, L. L. Brody, S. N. Coulter, K. R. Folger, A. Kas, K. Larbig, R. Lim, K. Smith, D. Spencer, G. K. Wong, Z. Wu, I. T. Paulsen, J. Reizer, M. H. Saier, R. E. Hancock, S. Lory, and M. V. Olson. 2000. Complete genome sequence of *Pseudomonas aeruginosa* PAO1, an opportunistic pathogen. Nature **406:**959–964.

46. **Touhami, A., M. H. Jericho, J. M. Boyd, and T. J. Beveridge.** 2006. Nanoscale characterization and determination of adhesion forces of *Pseudomonas aeruginosa* pili by using atomic force microscopy. J. Bacteriol. **188:**370–377.
47. **Vadillo-Rodriguez, V., H. J. Busscher, W. Norde, J. de Vries, and H. C. van der Mei.** 2003. On relations between microscopic and macroscopic physicochemical properties of bacterial cell surfaces: an AFM study on *Streptococcus mitis* strains. Langmuir **19:**2372–2377.
48. **van Oss, C. J.** 1994. Interfacial forces in aqueous media. Marcel Dekker, New York, NY.
49. **Walker, S. L., J. A. Redman, and M. Elimelech.** 2004. Role of cell surface lipopolysaccharides in *Escherichia coli* K12 adhesion and transport. Langmuir **20:**7736–7746.
50. **Whiteley, M., M. R. Parsek, and E. P. Greenberg.** 2000. Regulation of quorum sensing by RpoS in *Pseudomonas aeruginosa*. J. Bacteriol. **182:**4356–4360.
51. **Williams, V., and M. Fletcher.** 1996. *Pseudomonas fluorescens* adhesion and transport through porous media are affected by lipopolysaccharide composition. Appl. Environ. Microbiol. **62:**100–104.
52. **Wozniak, D. J., T. J. O. Wyckoff, M. Starkey, R. Keyser, P. Azadi, G. A. O'Toole, and M. R. Parsek.** 2003. Alginate is not a significant component of the extracellular polysaccharide matrix of PA14 and PAO1 *Pseudomonas aeruginosa* biofilms. Proc. Natl. Acad. Sci. USA **100:**7907–7912.